

THE CONSTRUCTION OF DOUBLY PERIODIC MINIMAL SURFACES VIA BALANCE EQUATIONS

By PETER CONNOR and MATTHIAS WEBER

Abstract. Using Traizet's regeneration method, we prove the existence of many new 3-dimensional families of embedded, doubly periodic minimal surfaces. All these families have a foliation of \mathbb{R}^3 by vertical planes as a limit. In the quotient, these limits can be realized conformally as noded Riemann surfaces, whose components are copies of \mathbb{C}^* with finitely many nodes. We derive the balance equations for the location of the nodes and exhibit solutions that allow for surfaces of arbitrarily large genus and number of ends in the quotient.

1. Introduction. A minimal surface M is called *doubly periodic* if it is invariant under two linearly independent orientation-preserving translations in euclidean space, which we can assume to be horizontal. The first such example was discovered by Scherk [11].

We denote the 2-dimensional lattice generated by the maximal group of such translations by Λ . If the quotient M/Λ is complete, properly embedded, and of finite topology, Meeks and Rosenberg [8] have shown that the quotient has a finite number of annular top and bottom ends which are asymptotic to flat annuli.

There are two cases to consider: either the top and bottom ends are parallel, or not. By results of Hauswirth and Traizet [3], a *non-degenerate* such surface is a smooth point of a moduli space of dimensions 1 in the non-parallel and 3 in the parallel case.

Moreover, Meeks and Rosenberg [8] have shown that in the parallel case, the number of top and bottom ends is equal to the same even number.

Lazard-Holly and Meeks [6] have shown that the doubly periodic Scherk surfaces are the only embedded doubly periodic surfaces of genus 0. In particular, the case of parallel ends does not occur for this genus.

For genus 1, there is an example of Karcher with orthogonal ends as well as a 3-dimensional family of such surfaces with parallel ends by Karcher [5] and Meeks-Rosenberg [7]. Moreover, Pérez, Rodríguez and Traizet [9] have shown that any doubly periodic minimal surface of genus one with parallel ends belongs to this family.

Douglas [2] and independently Baginsky and Batista [1] have shown that the Karcher example can be deformed to a 1-parameter family by changing the angle

Manuscript received November 24, 2009; revised June 10, 2010.

American Journal of Mathematics 134 (2012), 1275–1301. © 2012 by The Johns Hopkins University Press.

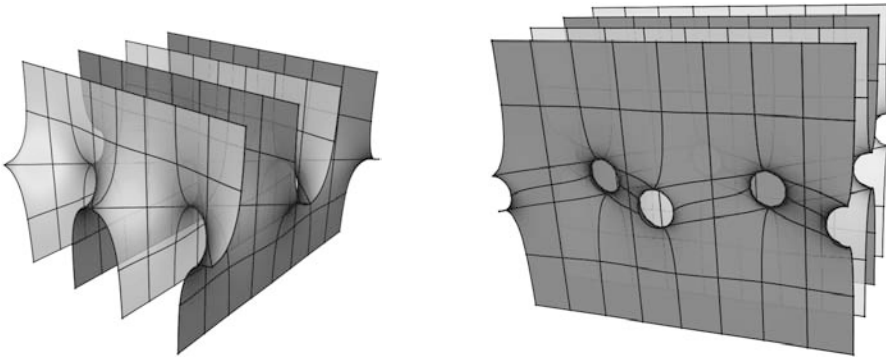


Figure 1. Scherk's surface and a Karcher-Meeks-Rosenberg surface.

between the ends. The family limits in the translation invariant helicoid with handles [4, 13]

For higher genus, only a few examples and families have been known so far:

In the non-parallel case, Weber and Wolf [14] have constructed examples of arbitrary genus, generalizing Karcher's example of genus 1.

Wei found a 1-parameter family of examples of genus 2 with parallel ends [15]. This family has been generalized considerably by Rossman, Thayer and Wohlgemuth [10] to allow for more ends. Rossman, Thayer, and Wohlgemuth did also construct an example with genus 3.

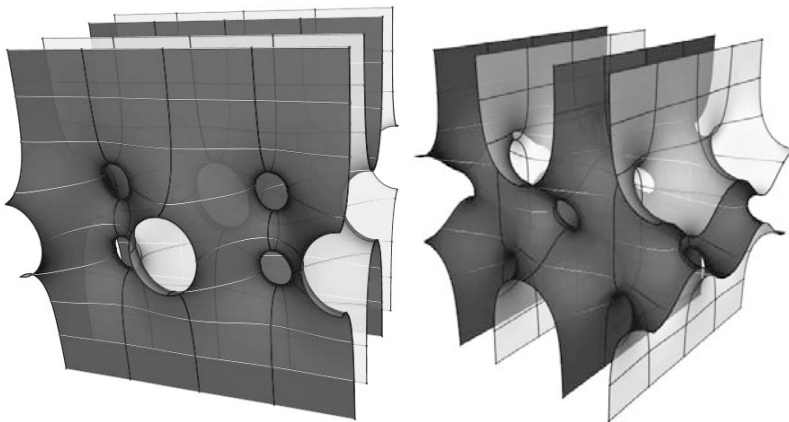


Figure 2. Genus two Wei surface and genus two RTW surface.

Our goal is to prove:

THEOREM 1.1. *For any genus $g \geq 1$ and any even number $N \geq 2$, there are 3-dimensional families of complete, embedded, doubly periodic minimal surfaces with parallel ends in euclidean space of genus g and N top and N bottom ends in the quotient by the maximal group of translations.*

Thus all topological types permitted by the results of Meeks and Rosenberg actually occur.

Figure 3 shows two translational copies in each direction of an example of genus 7.

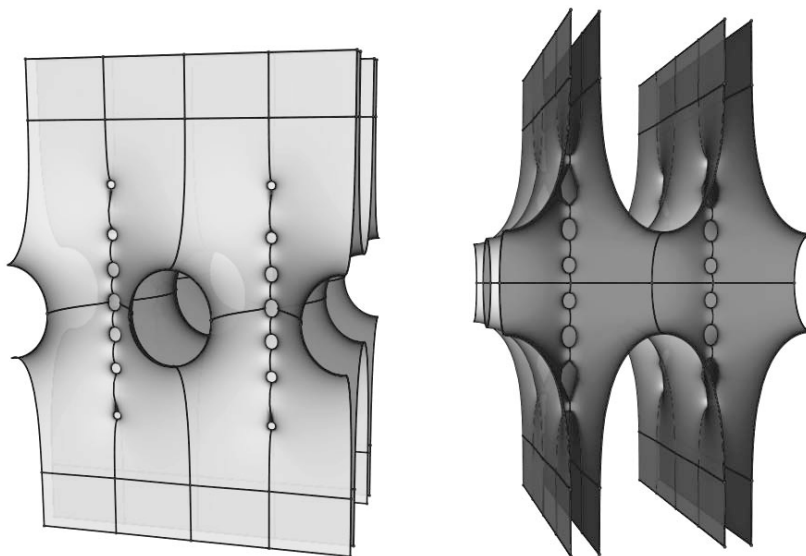


Figure 3. Two views of a genus 7 surface.

The methods used in this paper are an adaptation of Traizet's techniques developed in [12]. There, Traizet constructs singly periodic minimal surfaces akin to Riemann's examples which limit in a foliation of euclidean space by horizontal planes. Near the limit, the surfaces look like a collection of parallel planes joined by catenoidal necks. In the limit, these necks develop into nodes so that the quotient surface becomes a noded Riemann surface. The components of the smooth part are punctured spheres, where the punctures have to satisfy Traizet's balance equations. Vice versa, given a finite collection of punctured spheres where the punctures satisfy the balance equations and are non-degenerate in a suitable sense, Traizet constructs a moduli space of Riemann surfaces which forms an open neighborhood of the noded surface. On these Riemann surfaces, he constructs Weierstrass data and solves the period problem using the implicit function theorem.

We will closely follow Traizet's paper, indicating all differences.

The paper is organized as follows: in Section 2, we state the results. In Section 3, we give examples. The main theorem is proven in sections 4 through 8. We prove the embeddedness of our surfaces and show they satisfy certain properties in Section 8.

Acknowledgment. We would like to thank the referee for many helpful comments.

2. Results. In this section, we will state precise formulations of our main theorems and introduce the relevant notation.

2.1. Description of the surfaces and its properties. Our goal is to construct three-dimensional families of embedded doubly periodic minimal surfaces M of arbitrary genus and with an even number N pairs of parallel annular ends in the quotient. The surfaces will depend on a small real parameter t (produced by the implicit function theorem) and a complex parameter T explained below.

In contrast to the introduction, we will choose the ends to be horizontal: This allows us to follow the notation and set-up of [12] more closely.

Denote the maximal group of orientation preserving translations of M by Λ . This group will contain a cyclic subgroup of horizontal translations. Denote one of its generators by \mathcal{T} .

By rotating and scaling the surface, we can assume that $\mathcal{T} = (0, 2\pi, 0)$. We will identify the horizontal (x_1, x_2) -plane with the complex plane \mathbb{C} using $z = x_1 + ix_2$. Note that the horizontal planar ends become flat annular ends in the quotient. Label a non-horizontal generator of Λ by \mathcal{T}_t . For $t \rightarrow 0$, \mathcal{T}_t will converge to a horizontal vector \bar{T} , where T is an arbitrary complex parameter. The conjugation is due to orientation issues that will become clear later on.

Also, order the ends by height and label them 0_k and ∞_k , with $k \in \mathbb{Z}$. Most of our work takes place on the quotient surfaces. There, the ends will be labeled 0_k and ∞_k as well, with $k = 1, \dots, N$ for some even integer N .

Our surfaces will have two additional properties.

Property 2.1. The quotient surface $\tilde{M}_t = M_t/\Lambda$ is a union of the following types of domains: for each pair of ends $E_k = \{0_k, \infty_k\}$, $k = 1, \dots, N$, there is an unbounded domain $E_{k,t} \subset \tilde{M}_t$ containing the ends 0_k and ∞_k that is a graph over a domain in $\mathbb{C}/(2\pi i\mathbb{Z})$ with $n_k + n_{k-1}$ topological disks removed.

$\tilde{M}_t - (E_{k,t} \cup E_{k+1,t})$ consists of n_k bounded annular components $C_{k,i,t}$ on which the Gauss map is one-to-one, called *catenoidal necks*.

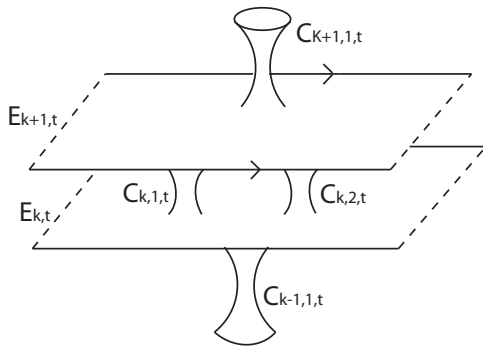


Figure 4. Annular regions and catenoid-shaped necks.

Property 2.2. There is a non-horizontal period \mathcal{T}_t such that as $t \rightarrow 0$:

- (1) The nonhorizontal period \mathcal{T}_t converges to a (possibly 0) horizontal vector \bar{T} .
- (2) The surfaces limit in a foliation of \mathbb{R}^3 by parallel planes.
- (3) The necksize of each annular component $C_{k,i,t}$ shrinks to 0, and the center of the neck $C_{k,i,t}$ converges to a point $\tilde{p}_{k,i}$.
- (4) The underlying Riemann surfaces limit in a noded Riemann surface consisting of N copies of $\mathbb{C}/(2\pi i\mathbb{Z})$, with nodes at points $\tilde{p}_{k,i}$.

Note that when we draw a model of \tilde{M}_t , the $E_{k,t}$ components should have the shape of an infinite annulus. As this is impossible to draw, we model the $E_{k,t}$ components with infinite flat cylinders.

After rotating the KMR and Wei’s surfaces so that the ends are horizontal, the behavior of both families near one of their limits fits the description given above.

2.2. Forces and balance equations. The location of the nodes $\tilde{p}_{k,i}$ introduced above is not arbitrary but governed by a system of algebraic equations. For convenience, we will identify $\mathbb{C}/(2\pi i\mathbb{Z})$ with \mathbb{C}^* via the exponential function and work with the latter. In particular, the nodes $\tilde{p}_{k,i}$ from the previous section will be determined as $\tilde{p}_{k,i} = \log(p_{k,i})$.

Consider N copies of \mathbb{C}^* , labeled \mathbb{C}_k^* for $k = 1, \dots, N$. On each \mathbb{C}_k^* , place n_k points $p_{k,1}, \dots, p_{k,n_k}$. Extend this definition of $p_{k,i}$ for any integer k by making it periodic with respect to a horizontal vector T in the sense that $p_{k+N,i} = p_{k,i}e^T$ for $k = 1, \dots, N$ and $i = 1, \dots, n_k$, with $n_{k+N} = n_k$. The difference between our $p_{k,i}$ terms and the ones in [12] is that the periodic condition in [12] is given by $\tilde{p}_{k+N,i} = \tilde{p}_{k,i} + T$. This is being consolidated by using the quotient map $\exp : \mathbb{C} \mapsto \mathbb{C}^*$. Thus, when we look at pictures of our surfaces, the nodes are really located at $\tilde{p}_{k,i}$ and are subject to the period vector T .

This set of points must satisfy a balancing condition given in terms of the following force equations.

Definition 2.1. The force exerted on $p_{k,i}$ by the other points in $\{p_{k,i}\}$ is defined by

$$\begin{aligned}
 F_{k,i} := & \sum_{j \neq i} \frac{p_{k,i} + p_{k,j}}{n_k^2 (p_{k,i} - p_{k,j})} - \sum_{j=1}^{n_{k+1}} \frac{p_{k,i} + p_{k+1,j}}{2n_k n_{k+1} (p_{k,i} - p_{k+1,j})} \\
 & - \sum_{j=1}^{n_{k-1}} \frac{p_{k,i} + p_{k-1,j}}{2n_k n_{k-1} (p_{k,i} - p_{k-1,j})}.
 \end{aligned}$$

Definition 2.2. The configuration $\{p_{k,i}\}$ is called a *balanced configuration* if $F_{k,i} = 0$ for $k = 1, \dots, N$ and $i = 1, \dots, n_k$.

Note that while the force equations do not seem to contain the parameter T , it enters the picture implicitly as the $p_{k,i}$ are assumed to form a T -periodic set.

Definition 2.3. Let $m = \sum_{i=1}^N n_k$ and F and p be the vectors in $\mathbb{C}^m = \mathbb{R}^{2m}$ whose components are made up of the $F_{k,i}$ and $p_{k,i}$ respectively. The balanced configuration $\{p_{k,i}\}$ is said to be *non-degenerate* if the differential of the map $p \mapsto F$ has rank $2(m - 1)$.

The differential of the map $p \mapsto F$ cannot have full rank $2m$ because

$$\sum_{k=1}^N \sum_{i=1}^{n_k} F_{k,i} = 0.$$

This holds whether or not the configuration $\{p_{k,i}\}$ is balanced.

Observe also that whenever we have a solution p for the balance equations, λp will also be a solution for any $\lambda \in \mathbb{C}^*$.

Now, we can state our main result.

THEOREM 2.1. *If $\{p_{k,i}\}$ is a non-degenerate balanced configuration then there exists a corresponding three-dimensional family of embedded doubly periodic minimal surfaces satisfying Properties 2.1 and 2.2, with genus*

$$g = 1 + \sum_{k=1}^N (n_k - 1),$$

and with $2N$ horizontal ends.

Our Main Theorem 1.1 will follow from this theorem and the non-degeneracy of the balance configurations of Proposition 3.2.

3. Examples. In this section, we will discuss examples of non-degenerate balanced configurations.

3.1. Adding handles to Wei’s genus two examples. In all known instances of Traizet’s regeneration technique, the simplest non-trivial configurations are given as the roots of special polynomials that satisfy a hypergeometric differential equation. So far, there is no explanation of this phenomenon, neither a general understanding of the more complicated solutions of the balance equations. In the case at hand, the crucial polynomials are

$$p_n(z) = \sum_{k=0}^n \binom{n}{k}^2 z^k.$$

They are related to the classical Legendre polynomials $L_n(z)$ by

$$p_n(z) = (1 - z)^n L_n\left(\frac{1 + z}{1 - z}\right),$$

as can be seen by comparing the differential equations for these polynomials. As $L_n(z)$ has n distinct roots in the interval $(-1, 1)$, our polynomials $p_n(z)$ have n distinct real roots $a_k < 0$.

PROPOSITION 3.1. *Let $n \in \mathbb{N}$ and a_1, a_2, \dots, a_n be the roots of the polynomial $p_n(z)$. Then the following configuration is balanced and non-degenerate: $N = 2$, $n_1 = 1$, $n_2 = n$, $p_{1,1} = 1$, $p_{2,i} = a_i$ for $i = 1, \dots, n$, and $T = 0$.*

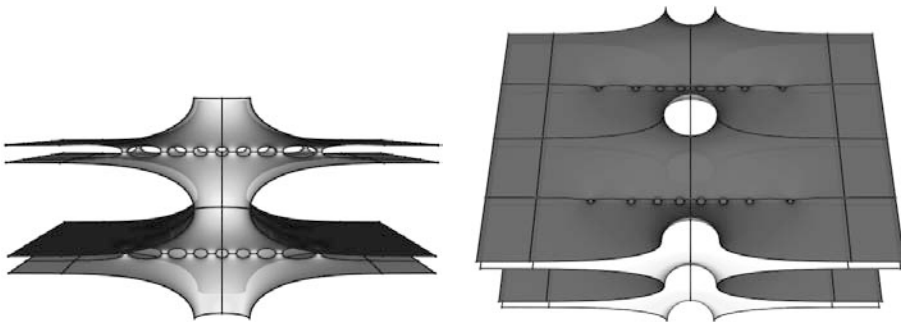


Figure 5. Genus 8 surface. The locations of the six small necks correspond to the roots of the polynomial $p_8(z) = z^8 + 64z^7 + 784z^6 + 3136z^5 + 4900z^4 + 3136z^3 + 784z^2 + 64z + 1$.

Proof. In this case, the balance equations are given by the following equations.

$$F_{1,1} = - \sum_{j=1}^n \frac{1 + a_j}{n(1 - a_j)}$$

$$F_{2,i} = \sum_{j \neq i} \frac{a_i + a_j}{n^2(a_i - a_j)} + \frac{1 + a_i}{n(1 - a_i)}$$

Observe first that the polynomials p_n satisfy the hypergeometric differential equation

$$z(1 - z)p_n''(z) + (1 + (2n - 1)z)p_n'(z) - n^2p_n(z) = 0.$$

Furthermore,

$$p_n(z) = z^n p_n(1/z)$$

Thus, for $n = 2k$, the roots will be $a_1, \dots, a_k, 1/a_1, \dots, 1/a_k$ and for $n = 2k + 1$, the roots will be $a_1, \dots, a_k, 1/a_1, \dots, 1/a_k, -1$. Hence, $F_{1,1} = 0$ by symmetry.

Since p_n only has simple zeroes, for each zero a_k we get the following equation.

$$p_n''(a_k) = 2p_n'(a_k) \sum_{j \neq k} \frac{1}{a_k - a_j}.$$

Plugging this into the hypergeometric differential equation for p_n , we get that

$$0 = 2a_k(1 - a_k) \sum_{j \neq k} \frac{1}{a_k - a_j} + 1 + (2n - 1)a_k.$$

This implies easily that $F_{2,k} = 0$ for $1 \leq k \leq n$, and so the given configuration is balanced $\forall n \in \mathbb{N}$.

To show that the configuration is non-degenerate, let M be the matrix with entries

$$M_{i,j} = \frac{\partial F_{2,i}}{\partial p_{2,j}}.$$

Then

$$M_{i,i} = \sum_{k \neq i} \frac{-2a_k}{n^2(a_i - a_k)^2} + \frac{2}{n(1 - a_i)^2}$$

and, if $i \neq j$,

$$M_{i,j} = \frac{2a_i}{n^2(a_i - a_j)^2}.$$

Thus,

$$\begin{aligned} \sum_{i \neq j} |M_{i,j}| &= \sum_{i \neq j} \frac{-2a_i}{n^2(a_i - a_j)^2} \\ &= \sum_{i \neq j} \frac{-2a_i}{n^2(a_j - a_i)^2} \\ &= M_{j,j} - \frac{2}{n(1 - a_j)^2} \\ &< M_{j,j} \end{aligned}$$

for $j = 1, \dots, n$. Hence, M is invertible and the differential of F has rank n . Thus, this configuration is non-degenerate. □

Remark 3.1. In the case $n = 1$ we obtain $a_1 = -1$. This balance configuration corresponds to the Karcher-Meeks-Rosenberg family [5, 7] of genus 1 doubly periodic minimal surfaces with parallel ends.

3.2. Combining non-degenerate balanced configurations. The next proposition requires two new definitions. They are adjustments on similar terms from [12]. Let $F_{k,i}^+$ be the sum of the forces exerted by the $p_{k+1,j}$ terms on $p_{k,i}$ and $F_{k,i}^-$ be the sum of the forces exerted by the $p_{k-1,j}$ terms on $p_{k,i}$, i.e.,

$$F_{k,i}^+ = \sum_{j=1}^{n_{k+1}} \frac{p_{k,i} + p_{k+1,j}}{2n_k n_{k+1} (p_{k,i} - p_{k+1,j})} - \frac{(-1)^k}{2n_k}$$

and

$$F_{k,i}^- = \sum_{j=1}^{n_{k-1}} \frac{p_{k,i} + p_{k-1,j}}{2n_k n_{k-1} (p_{k,i} - p_{k-1,j})} - \frac{(-1)^{k+1}}{2n_k}.$$

PROPOSITION 3.2. *Let $p_{k,i}$ and $p'_{k,i}$ be two balanced configurations. Assume that:*

- (1) $n_1 = n'_1 = 1$,
- (2) $p_{1,1} = p'_{1,1} = 1$,
- (3) $F_{1,1}^+ = F'_{1,1}^+ \neq 0$.

Define $p''_{k,i}$ as follows:

$$\begin{aligned} \forall k \in \{1, \dots, N\}, n''_k &= n_k \text{ and } p''_{k,i} = p_{k,i} \\ \forall k \in \{1, \dots, N'\}, n''_{k+N} &= n'_k \text{ and } p''_{k+N,i} = p'_{k,i} e^T \\ \forall k \in \mathbb{Z}, p''_{k+N+N',i} &= p''_{k,i} e^{T+T'}. \end{aligned}$$

The configuration $p''_{k,i}$ is periodic with $N'' = N + N'$ and $T'' = T + T'$. Then:

- (1) The configuration $p''_{k,i}$ is balanced.
- (2) Suppose $p_{k,i}$ and $p'_{k,i}$ are non-degenerate and that $T = T' = 0$. Then $p''_{k,i}$ is non-degenerate.

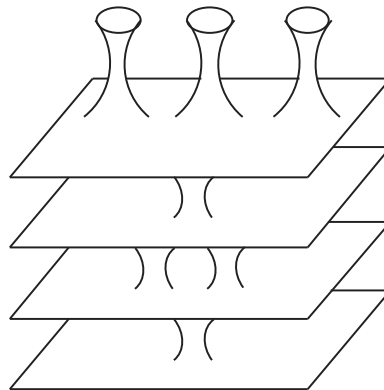


Figure 6. Surface corresponding to non-degenerate balanced configuration with $n = 2$, and $n' = 3$.

We can use Proposition 3.2 to inductively construct non-degenerate balanced configurations for any positive even integer N , with $n_k = 1$ when k is odd. In fact, $p_{k,1} = 1$ when k is odd. When k is even, the $p_{k,i}$ will correspond to the roots of the polynomial $p_{n_k}(z)$ from Proposition 3.1.

Proof. The proof of part one of this proposition is exactly the same as the proof of part one of Proposition 3 in [12].

As for the proof of part two, suppose that there is a variation $p''_{k,i}(t)$ of (not necessarily balanced) configurations with $p''_{k,i}(0) = p''_{k,i}$ and $T''(t) = 0$ such that

$$\frac{d}{dt}F(p''(t))|_{t=0} = 0.$$

By scaling, we can assume that $p''_{11}(t) = p_{11} = 1$. This removes the trivial part of the kernel of dF . We thus have to show that

$$\frac{d}{dt}p''(t)|_{t=0} = 0.$$

Define $p_{k,i}(t) = p''_{k,i}(t)$ for $k = 1, \dots, N$. We make the $p_{k,i}(t)$ periodic by insisting on $p_{k+N,i}(t) = p_{k,i}(t)$ for all $k \in \mathbb{Z}$.

Then, for $k = 2, \dots, N$,

$$\frac{d}{dt}F_{k,i}(p(t))|_{t=0} = 0.$$

As the sum of all forces is $= 0$ and $n_1 = 1$, this holds in fact for all k .

Now, $p_{k,i}(t)$ and $p_{k,i}$ are periodic with the same period $T = 0$ and both satisfy the balance equations (for $t = 0$). Furthermore, for $t = 0$, $p_{k,i}(0) = p_{k,i}$ and $p_{11}(0) = p_{11} = 1$. Since $p_{k,i}$ is nondegenerate, it follows that $\frac{d}{dt}p_{k,i}(t)|_{t=0} = 0$ and thus $\frac{d}{dt}p''_{k,i}(t)|_{t=0} = 0$ for $k = 1, \dots, N$. Similarly, using the non-degeneracy of the $p'_{k,i}$ one shows that $\frac{d}{dt}p''_{k,i}(t)|_{t=0} = 0$ for $k = N + 1, \dots, N + N'$. This establishes the non-degeneracy of the $p''_{k,i}$. \square

3.3. Other examples and non-examples.

Example 3.2. There exists a non-degenerate balanced configuration $\{p_{k,i}\}$ with $N = 2, n_1 = n_2 = 2$, and $T = 0$. However, the corresponding surface is a scaled version of the surface corresponding to the balanced configuration with $N = 2, n_1 = n_2 = 1$ and $T = 0$. Instead of a horizontal period of $2\pi i$, these surfaces have a horizontal period of πi .

Example 3.3. There exist at least two distinct non-degenerate balanced configurations $\{p_{k,i}\}$ with $N = 2, n_1 = 2, n_2 = 3$, and $T = 0$.

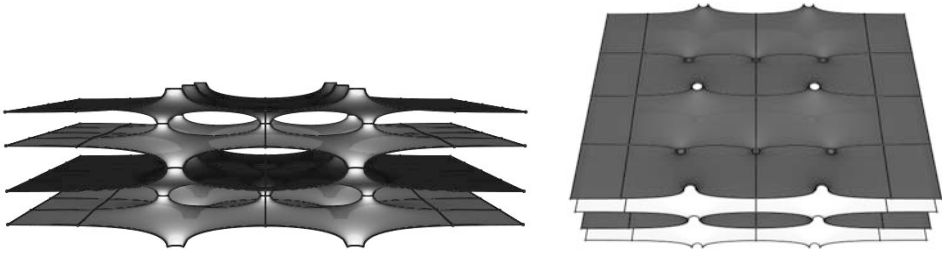


Figure 7. Side and top views of a genus four surface with $N = 2, n_1 = 2, n_2 = 3$.

The force equations corresponding to this setup are

$$F_{1,i} = (-1)^i \frac{p_{1,1} + p_{1,2}}{4(p_{1,2} - p_{1,1})} - \sum_{j=1}^3 \frac{p_{1,i} + p_{2,j}}{6(p_{1,i} - p_{2,j})}$$

for $i = 1, 2$ and

$$F_{2,i} = \sum_{j \neq i} \frac{p_{2,i} + p_{2,j}}{9(p_{2,i} - p_{2,j})} - \sum_{j=1}^2 \frac{p_{2,i} + p_{1,j}}{6(p_{2,i} - p_{1,j})}$$

for $i = 1, 2, 3$.

(1) Let $a_1 = 4 + 2\sqrt{5} + \sqrt{35 + 16\sqrt{5}}$ and $a_2 = \frac{1}{2}(-17 - 9\sqrt{5} - \sqrt{690 + 306\sqrt{5}})$, and let $p_{1,1} = a_1, p_{1,2} = 1/a_1, p_{2,1} = a_2, p_{2,2} = -1$, and $p_{2,3} = 1/a_2$. Then $F_{k,i} = 0$ for $k = 1, 2$ and $i = 1, \dots, n_k$, and so $\{p_{k,i}\}$ is a balanced configuration.

(2) Let $b_1 = 4 - 2\sqrt{5} - i\sqrt{-35 + 16\sqrt{5}}$ and $b_2 = \frac{1}{2}(-17 + 9\sqrt{5} - \sqrt{690 - 306\sqrt{5}})$, and let $p_{1,1} = b_1, p_{1,2} = 1/b_1, p_{2,1} = b_2, p_{2,2} = -1$, and $p_{2,3} = 1/b_2$. Then $F_{k,i} = 0$ for $k = 1, 2$ and $i = 1, \dots, n_k$, and so $\{p_{k,i}\}$ is a balanced configuration.

In both cases, the configurations are non-degenerate by a numerical computation.

Numerical evidence suggests:

CONJECTURE 3.3. *There exists a non-degenerate balanced configuration $\{p_{k,i}\}$ with $N = 2, n_1 = 2, n_2 = 2k - 1$, and $T = 0$ for $k \in \mathbb{N}$.*

Remark 3.4. In contrast to [12], all our examples of balance configurations above have horizontal period $T = 0$. It is possible to solve the balance equations also for $T \neq 0$. However, the solutions become much more complicated and we have not been able to use them to construct surface families that are provably distinct from the ones we obtain for $T = 0$.

4. Weierstrass Data. We begin the proof of Theorem 1 by parametrizing a set of Riemann surfaces and Weierstrass data that are candidates for the minimal surfaces we want to construct. The construction is almost exactly the same as in [12]. The main difference is our definition of the Gauss map G . We repeat the details for the convenience of the reader.

Let $\bar{\mathbb{C}}_k = \bar{\mathbb{C}}$ for $k = 1, \dots, N$, and for each $k \in \{1, \dots, N\}$ let $G_k : \bar{\mathbb{C}}_k \rightarrow \bar{\mathbb{C}}$ be the meromorphic function defined by

$$G_k(z) = \delta_k z \left(\sum_{i=1}^{n_k} \frac{\alpha_{k,i}}{z - a_{k,i}} - \sum_{i=1}^{n_{k-1}} \frac{\beta_{k,i}}{z - b_{k,i}} \right)$$

where $\delta_k \in (0, \infty)$, the poles $a_{k,i}$ and $b_{k,i}$ are distinct non-zero complex numbers, and the $\alpha_{k,i}$ and $\beta_{k,i}$ are non-zero complex numbers such that

$$\sum_{i=1}^{n_k} \alpha_{k,i} = \sum_{i=1}^{n_{k-1}} \beta_{k,i} = 1.$$

The first equality ensures that $G_k(z)$ has a zero at ∞ . The zeroes at 0 and ∞ are needed to ensure that the Gauss map is vertical at the annular ends. The δ_k terms will be used to ensure that the periods at the ends are the same. In [12], the corresponding map is $g_k(z) = \frac{G_k(z)}{\delta_k z}$.

Let $\alpha_k = (\alpha_{k,1}, \dots, \alpha_{k,n_k})$ and $\alpha = (\alpha_1, \dots, \alpha_N)$, and define β, γ, a and b in the same way. Let $\delta = (\delta_1, \dots, \delta_N)$ and $X = (\alpha, \beta, \delta, \gamma, a, b)$. The set X is our set of parameters used to construct the Riemann surfaces and Weierstrass data.

The surfaces we are constructing have n_k catenoid-shaped necks between the k and $k + 1$ levels. In order to achieve this, we use the functions G_k to create coordinates near each pole and identify an annulus centered at $a_{k,i} \in \bar{\mathbb{C}}_k$ with an annulus centered at $b_{k+1,i} \in \bar{\mathbb{C}}_{k+1}$ for $k = 1 \dots, N$ and $i = 1, \dots, n_k$ using the following procedure.

The function $v_{k,i} = 1/G_k$ has a simple zero at $a_{k,i}$. Thus, there exists $\epsilon > 0$ such that $v_{k,i}$ is a biholomorphic map from a neighborhood of $a_{k,i} \in \bar{\mathbb{C}}_k$ to the disk $D_\epsilon(0)$. In this manner, $v = v_{k,i}$ is a complex coordinate in a neighborhood of $a_{k,i}$. Similarly, $w = w_{k+1,i} = 1/G_{k+1}$ is a biholomorphic map from a neighborhood of $b_{k+1,i} \in \bar{\mathbb{C}}_{k+1}$ to the disk $D_\epsilon(0)$. Thus, for each pair $a_{k,i}$ and $b_{k+1,i}$ we get the pair of coordinates $v = v_{k,i}$ and $w = w_{k+1,i}$.

Choose a positive real number r with $r \in (0, \epsilon^2)$ and remove the disks $|v| \leq \frac{r}{\epsilon}$ and $|w| \leq \frac{r}{\epsilon}$ from $\bar{\mathbb{C}}_k$ and $\bar{\mathbb{C}}_{k+1}$, respectively. Then, we create a conformal model of the catenoid-shaped neck by identifying the points in $\bar{\mathbb{C}}_k$ satisfying

$$\frac{r}{\epsilon} < |v| < \epsilon$$

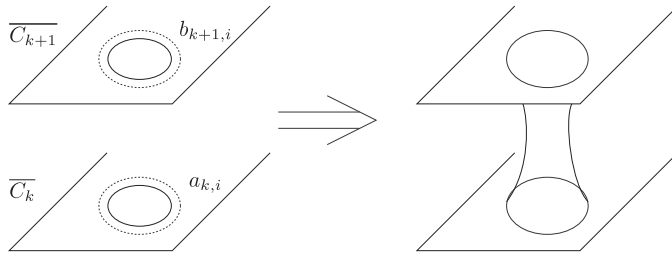


Figure 8. Gluing construction.

with points in \bar{C}_{k+1} satisfying

$$\frac{r}{\epsilon} < |w| < \epsilon$$

by the equation

$$vw = r.$$

Let Σ be the compact Riemann surface created by repeating this procedure for each $k = 1, \dots, N$ and $i = 1, \dots, n_k$. Note that the index k is modulo N . Thus, the gluing between \bar{C}_N and \bar{C}_{N+1} is really a gluing between \bar{C}_N and \bar{C}_1 .

Denote by Σ^* the surface obtained by removing the points 0_k and ∞_k from Σ for all k . When $r = 0$, define Σ as the disjoint union $\bar{C}_1 \cup \bar{C}_2 \cup \dots \cup \bar{C}_N$. This is the underlying Riemann surface for our minimal surface candidates.

Next, the Gauss map $G : \Sigma \rightarrow \bar{C}$ is defined by

$$(1) \quad G(z) = \begin{cases} \sqrt{r}G_k(z) & \text{if } z \in \bar{C}_k, k \text{ even,} \\ \frac{1}{\sqrt{r}G_k(z)} & \text{if } z \in \bar{C}_k, k \text{ odd.} \end{cases}$$

If k is even, then $G = \sqrt{r}/v$ on \bar{C}_k and $G = w/\sqrt{r}$ on \bar{C}_{k+1} . If k is odd, then $G = v/\sqrt{r}$ on \bar{C}_k and $G = \sqrt{r}/w$ on \bar{C}_{k+1} . Therefore, the relation $vw = r$ implies that G is well-defined on Σ .

Before defining our height differential η , we need to choose a basis of the homology of Σ . Define $A_{k,i}$ to be the circle $|v_{k,i}| = \epsilon$ in \bar{C}_k oriented positively. The construction of Σ implies that this is homotopic to the circle $|w_{k+1,i}| = \epsilon$ oriented negatively. Choose $B_{k,i}, i \geq 2$, to be a closed curve in Σ such that $A_{k,1} \cdot B_{k,i} = -1, A_{k,i} \cdot B_{k,i} = 1, A_{m,n} \cdot B_{k,i} = 0$ if $m \neq k$, and $B_{k,i} \cdot B_{m,n} = 0$ if $(m,n) \neq (k,i)$. Finally, choose $B_{1,1}$ to be a closed curve such that $A_{k,1} \cdot B_{1,1} = 1$ for $k = 1, \dots, N$ and it does not intersect any of the above curves. Then a basis of $H_1(\Sigma)$ is given by the curves $A_{1,1}, B_{1,1}, A_{k,i}$, and $B_{k,i}$, with $k = 1, \dots, N$ and $i = 2, \dots, n_k$. Note that if we replace the $B_{1,i}$ curves by $B'_{1,i} = B_{1,i} + B_{1,1}$ then we get a canonical basis of $H_1(\Sigma)$.

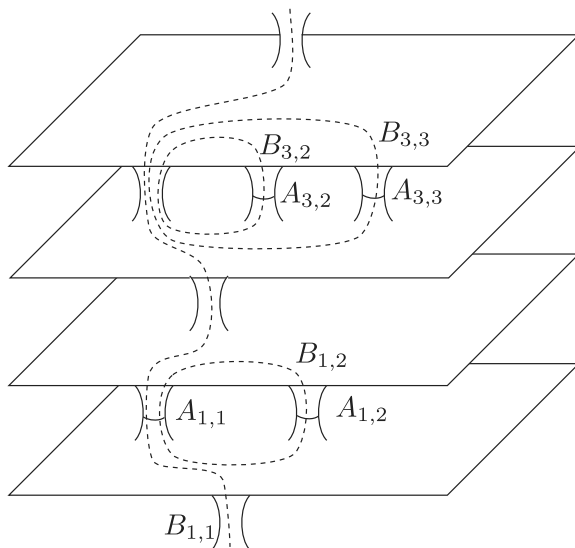


Figure 9. Labeling the cycles.

PROPOSITION 4.1. [12] Consider numbers $\gamma_{k,i}$, $k = 1, \dots, N$, $i = 1, \dots, n_k$ such that for any k ,

$$\sum_{i=1}^{n_k} \gamma_{k,i} = 1.$$

Then there exists a unique holomorphic 1-form η on Σ such that for any $k = 1, \dots, N$, $i = 1, \dots, n_k$,

$$\int_{A_{k,i}} \eta = 2\pi i \gamma_{k,i}.$$

The proof is the same as in the proof of Proposition 5 from Section 3.3 in [12].

We now have a space of Riemann surfaces and Weierstrass data that are candidates for the surfaces we want to construct. The parameters are given by (r, X) , and we will look at what happens when $r \rightarrow 0$.

5. Constraints on the Weierstrass data and period conditions. We parametrize the surface as

$$\psi(z) = \operatorname{Re} \int_{z_0}^z (\phi_1, \phi_2, \phi_3)$$

where $z_0 \in \Sigma$ is a base point, $\phi_1 = \frac{1}{2} \left(\frac{1}{G} - G \right) \eta$, $\phi_2 = \frac{i}{2} \left(\frac{1}{G} + G \right) \eta$, and $\phi_3 = \eta$. In order that (Σ, G, η) are the Weierstrass data of a complete, doubly periodic minimal surface with horizontal embedded ends, we need:

(1) For any $p \in \Sigma^*$, η has a zero at p if and only if G has either a zero or pole at p , with the same multiplicity. At each puncture 0_k and ∞_k , G has a zero or pole of order $n \geq 1$ and η has a zero of order $n - 1$.

(2) For any closed curve c on Σ^* , $\text{Re} \int_c \phi_j$ is an integral linear combination of two linearly independent vectors of \mathbb{R}^3 . We denote the set of these linear combinations by Λ .

As the zeroes and poles of G are the zeroes of the G_k , we can write condition (1) equivalently as

(1') The zeroes of η are the zeroes of $G_k dz/z$, $k = 1, \dots, N$, with the same multiplicity.

If condition (1) is satisfied then the 1-forms ϕ_1 and ϕ_2 have poles only at the punctures of Σ^* , and so condition (2) needs to be checked only for a canonical basis of the homology of Σ and for small loops around the punctures. Therefore we can rewrite the condition (2) as follows: Write $\phi = (\phi_1, \phi_2, \phi_3)$.

(2'.1) For any $k = 1, \dots, N$ and $i = 1, \dots, n_k$,

$$\text{Re} \int_{A_{k,i}} \phi = 0.$$

(2'.2) For any $k = 1, \dots, N$ and $i = 2, \dots, n_k$,

$$\text{Re} \int_{B_{k,i}} \phi = 0,$$

(2'.3)

$$\text{Re} \int_{B_{1,1}} \phi \in \Lambda.$$

(2'.4) For any $k = 1, \dots, N$,

$$\text{Re} \int_{\partial D_\epsilon(0_k)} \phi \in \Lambda.$$

(2'.5) For any $k = 1, \dots, N$,

$$\text{Re} \int_{\partial D_\epsilon(\infty_k)} \phi \in \Lambda.$$

If $\text{Re} \int_{A_{k,i}} \phi = 0$ and $\text{Re} \int_{\partial D_\epsilon(0_k)} \phi \in \Lambda$ for each k, i then the period condition at ∞_k is automatically satisfied by Cauchy's theorem. Observe that the period vectors $\text{Re} \int_{\partial D_\epsilon(0_k)} \phi$ and $\text{Re} \int_{\partial D_\epsilon(\infty_k)} \phi$ are necessarily horizontal, as $\eta = \phi_3$ is holomorphic at 0_k and ∞_k .

6. Height differential extends holomorphically to $r = 0$. The results of this section follow precisely as in [12]. Recall that when $r = 0$, we defined Σ as the disjoint union $\bar{C}_1 \cup \bar{C}_2 \cup \dots \cup \bar{C}_N$. The Gauss map is defined when $r = 0$ and depends holomorphically on r . We need the same to be true for the height differential. When $r = 0$, define η by $\eta = \eta_k$ on \bar{C}_k where η_k is the unique meromorphic 1-form on \bar{C}_k with simple poles at $a_{k,i}$ and $b_{k,i}$ with residues $\gamma_{k,i}$ and $-\gamma_{k-1,i}$, i.e.,

$$\eta_k = \left(\sum_{i=1}^{n_k} \frac{\gamma_{k,i}}{z - a_{k,i}} - \sum_{i=1}^{n_{k-1}} \frac{\gamma_{k-1,i}}{z - b_{k,i}} \right) dz.$$

Observe that our conditions ensure that η is holomorphic at 0_k and ∞_k for each k .

The next two propositions are from Section 4 in [12]. As our height differential is defined in the same way as in [12], the proofs of these propositions are the same.

PROPOSITION 6.1. [12] *Let $z \in \bar{C}_k$, $z \neq a_{k,i}$, $z \neq b_{k,i}$. Then $r \mapsto \eta(z)$ is holomorphic in a neighborhood of 0.*

PROPOSITION 6.2. [12] *Let $v = v_{k,i}$. On the domain $\frac{r}{\epsilon} < |v| < \epsilon$ of Σ , we have the formula*

$$\eta = f\left(v, \frac{r}{v}\right) \frac{dv}{v} = -f\left(\frac{r}{w}, w\right) \frac{dw}{w}$$

where f is a holomorphic function of two complex variables defined in a neighborhood of $(0, 0)$.

We can use propositions 6.1 and 6.2 to estimate the integrals of $\eta, G\eta$, and $1/G\eta$ on the homology cycles and on cycles around the punctures. These are necessary to solve the period problem when $r = 0$. As in [12], we will use a term $\text{holo}(r, X)$, meaning a holomorphic function in terms of (r, X) in a neighborhood of $(0, X_0)$.

PROPOSITION 6.3. [12]

$$\begin{aligned} \int_{A_{k,i}} G^{(-1)^k} \eta &= \sqrt{r} \left(2\pi i \text{res}_{a_{k,i}} G_k \eta_k + r \text{holo}(r, X) \right) \\ \int_{A_{k,i}} G^{(-1)^{k+1}} \eta &= \sqrt{r} \left(-2\pi i \text{res}_{b_{k+1,i}} G_{k+1} \eta_{k+1} + r \text{holo}(r, X) \right) \\ \int_{B_{k,i}} \eta &= (\gamma_{k,i} - \gamma_{k,1}) \log(r) + \text{holo}(r, X) \\ \int_{B_{k,i}} G^{(-1)^k} \eta &= \frac{1}{\sqrt{r}} \left(\int_{b_{k+1,i}}^{b_{k+1,1}} G_{k+1}^{-1} \eta_{k+1} + r \log(r) \text{holo}(r, X) + r \text{holo}(r, X) \right) \end{aligned}$$

$$\int_{B_{k,i}} G^{(-1)^{k+1}} \eta = \frac{1}{\sqrt{r}} \left(\int_{a_{k,1}}^{a_{k,i}} G_k^{-1} \eta_k + r \log(r) \text{holo}(r, X) + r \text{holo}(r, X) \right).$$

The proofs are the same as in [12, Section 5]. The following proposition takes care of the different nature of our annular ends compared to the planar ends on [12].

PROPOSITION 6.4.

$$\begin{aligned} \int_{\partial D_\epsilon(0_k)} G^{(-1)^k} \eta &= 0 \\ \int_{\partial D_\epsilon(0_k)} G^{(-1)^{k+1}} \eta &= \frac{1}{\sqrt{r}} \left(2\pi i \text{res}_0 \frac{1}{G_k} \eta_k + r \text{holo}(r, X) \right). \end{aligned}$$

Proof. First,

$$\int_{\partial D_\epsilon(0_k)} G^{(-1)^k} \eta = \sqrt{r} \int_{\partial D_\epsilon(0_k)} G_k \eta = 0$$

because $G_k \eta$ has no poles in a neighborhood of 0_k . Using proposition 6.1,

$$\begin{aligned} \int_{\partial D_\epsilon(0_k)} G^{(-1)^{k+1}} \eta &= \frac{1}{\sqrt{r}} \int_{\partial D_\epsilon(0_k)} \frac{1}{G_k} (\eta_k + r \text{holo}(r, X) dz) \\ &= \frac{1}{\sqrt{r}} \left(2\pi i \text{res}_{0_k} \frac{1}{G_k} \eta_k + r \text{holo}(r, X) \right). \end{aligned} \quad \square$$

7. Solving the period problem. We can attempt to solve the constraints on the Weierstrass data and the period problem by adjusting the variables (r, X) , and we will express this with a map \mathcal{F} . In fact, we will find solutions when $r = 0$. This allows us to take advantage of the asymptotic expansion of each of the periods at $r = 0$.

Let $\zeta_{k,i}$ be the zeroes of $\frac{1}{\delta_k z} G_k dz$ in $\overline{\mathbb{C}}_k$, $i = 1, \dots, n_k + n_{k-1} - 2$. Define

$$\mathcal{F}_{1,k,i} = \eta(\zeta_{k,i}).$$

Abbreviate $\mathcal{F}_{1,k} = (\mathcal{F}_{1,k,1}, \dots, \mathcal{F}_{1,k,n_k+n_{k-1}-2})$ and $\mathcal{F}_1 = (\mathcal{F}_{1,1}, \dots, \mathcal{F}_{1,N})$. The zeroes of $\frac{1}{\delta_k z} G_k dz$ can be thought of as the zeroes of a polynomial, and for now let us assume that they are all simple zeroes. Section 9 in [12] takes care of the case where $\frac{1}{\delta_k z} G_k dz$ may not only have simple zeroes, and applies here as well. As argued in [12], the simple zeroes of a polynomial depend analytically on its coefficients and, by Proposition 6.1, \mathcal{F}_1 depends analytically on (r, X) .

If $\mathcal{F}_1 = 0$ then η has at least a simple zero at each zero of G'_k . All the zeroes of $\frac{1}{\delta_k z} G_k dz$ are assumed to be simple, and so G has

$$\sum_{k=1}^N (n_k + n_{k-1} - 2) = 2 \sum_{k=1}^N n_k - 2N$$

zeroes and poles, counting multiplicity.

The number of zeroes of η is

$$\begin{aligned} 2 \text{genus}(\Sigma) - 2 &= 2 \left(1 + \sum_{k=1}^N (n_k - 1) \right) - 2 \\ &= 2 + 2 \sum_{k=1}^N n_k - 2N - 2 \\ &= 2 \sum_{k=1}^N n_k - 2N. \end{aligned}$$

Thus, the zeroes of η are precisely the $\zeta_{k,i}$.

The remaining components of the map \mathcal{F} deal with the period problem. The period condition $\text{Re} \int_{A_{k,i}} \eta = 0$ is taken care of by letting $\gamma_{k,i} \in \mathbb{R}$. This is simply due to how we defined η . From this moment on, assume that $\gamma_{k,i} \in \mathbb{R}$. Recall that

$$\text{Re} \int \phi_1 + i \text{Re} \int \phi_2 = \frac{1}{2} \left(\int G^{-1} \eta - \int G \eta \right).$$

With this equivalency in mind, we define

$$\begin{aligned} \mathcal{F}_{2,k,i} &= \frac{1}{\log r} \text{Re} \int_{B_{k,i}} \eta, \quad i = 2, \dots, n_k, \\ \mathcal{F}_{3,k,i} &= \sqrt{r} \left(\int_{B_{k,i}} G^{-1} \eta - \int_{B_{k,i}} G \eta \right), \quad i = 2, \dots, n_k, \\ \mathcal{F}_{4,k,i} &= \frac{(-1)^k}{\sqrt{r}} \left(\int_{A_{k,i}} G^{-1} \eta - \int_{A_{k,i}} G \eta \right), \quad i = 1, \dots, n_k, \\ \mathcal{F}_{5,k} &= 2\sqrt{r} \left(\int_{\partial D_\epsilon(0_k)} G^{-1} \eta - \int_{\partial D_\epsilon(0_k)} G \eta \right) + 2\pi i. \end{aligned}$$

Define the vectors $\mathcal{F}_2, \mathcal{F}_3$, and \mathcal{F}_4 as we defined \mathcal{F}_1 . Let $\mathcal{F}_5 = (\mathcal{F}_{5,1}, \mathcal{F}_{5,2}, \dots, \mathcal{F}_{5,N})$ and $\mathcal{F} = (\mathcal{F}_1, \mathcal{F}_2, \mathcal{F}_3, \mathcal{F}_4, \mathcal{F}_5)$. Note that the constraints of the Weierstrass data and the period problem listed in Section 3.2 are equivalent to $\mathcal{F} = 0$. Also, there is no need for \mathcal{F}_5 in [12].

The $\log r$ terms that show up in \mathcal{F} require us to express the variable r in terms of the variable t using the equation $r(t) = e^{-1/t^2}$ if $t \in \mathbb{R} \setminus \{0\}$ and $r(0) = 0$.

Otherwise, the map \mathcal{F} won't be differentiable at $r = 0$. Propositions 6.3 and 6.4 imply that \mathcal{F} is differentiable at $r = 0$.

The next proposition is essentially the same as Proposition 9 in [12]. The key difference is in the definition of $a_{k,i}$ and $b_{k,i}$. This difference plays out in the rest of the calculations of this section, which lead to the proof of the proposition. Recall also that the $p_{k,i}$ form a periodic set of points with $p_{k+N,i} = p_{k,i}e^T$. This introduces a similar, but more obfuscated periodicity of the $a_{k,i}$ and $b_{k,i}$ below.

Below, conj denotes the conjugation in \mathbb{C} .

PROPOSITION 7.1. *Let $\{p_{k,i}\}$ be a balanced configuration. Define X_o by:*

$$(2) \quad \begin{cases} \alpha_{k,i} = \gamma_{k,i} = \beta_{k+1,i} = 1/n_k, \\ a_{k,i} = (\text{conj}^k(p_{k,i}))^{(-1)^k}, \\ b_{k,i} = (\text{conj}^k(p_{k-1,i}))^{(-1)^k}. \end{cases}$$

Then $\mathcal{F}(0, X_o) = 0$. Also, if X is a solution to $\mathcal{F}(0, X) = 0$ then, up to some identifications, $X = X_o$ for some balanced configuration $\{p_{k,i}\}$. In addition, if $\{p_{k,i}\}$ is a non-degenerate balanced configuration then, up to some identifications, $D_2\mathcal{F}(0, X_o)$ is an isomorphism. By the implicit function theorem, for t in a neighborhood of 0, there exists a unique $X(t)$ in a neighborhood of X_o such that $\mathcal{F}(t, X(t)) = 0$.

The Weierstrass data given by each unique $X(t)$ is the map of an immersed doubly periodic minimal surface with embedded planar ends. The rest of this section contains the proof of Proposition 7.1.

7.1. Solving the equation $\mathcal{F}_1 = 0$. Assume $r = 0$. $\mathcal{F}_{1,k} = 0$ is equivalent to: $G_k dz$ and η_k have the same zeroes on \tilde{C}_k . Since they already have the same poles they are proportional. By normalization, $\eta_k = \frac{1}{\delta_{kz}} G_k dz$. Thus, $\mathcal{F}_1 = 0$ is equivalent to $\alpha_{k,i} = \gamma_{k,i}$ and $\beta_{k,i} = \gamma_{k-1,i}$.

From this moment on, assume that $\mathcal{F}_1 = 0$ so that $r = 0 \Rightarrow \eta_k = \frac{1}{\delta_{kz}} G_k dz$.

7.2. Solving the equation $\mathcal{F}_2 = 0$. Using Proposition 6.3,

$$\begin{aligned} \mathcal{F}_{2,k,i} &= \frac{1}{\log(r)} \text{Re} \int_{B_{k,i}} \eta \\ &= \frac{1}{\log(r)} \text{Re} ((\gamma_{k,i} - \gamma_{k,1}) \log(r) + \text{holo}(r, X)) \\ &= \gamma_{k,i} - \gamma_{k,1} + \frac{\text{Re}(\text{holo}(r, X))}{\log(r)}. \end{aligned}$$

When $r = 0$, $\mathcal{F}_{2,k,i} = \gamma_{k,i} - \gamma_{k,1}$. Thus, $\mathcal{F}_2 = 0 \Rightarrow \gamma_{k,i} = \gamma_{k,1} \forall i \Rightarrow \gamma_{k,i} = \frac{1}{n_k} \forall i$.

7.3. Solving the equation $\mathcal{F}_3 = 0$. Using Proposition 6.3,

$$\begin{aligned} \mathcal{F}_{3,k,i} &= \sqrt{r} \left(\overline{\int_{B_{k,i}} G^{-1}\eta - \int_{B_{k,i}} G\eta} \right) \\ &= (-1)^k \text{conj}^k \left(\int_{a_{k,1}}^{a_{k,i}} G_k^{-1}\eta_k + r \log(r) \text{holo}(r, X) + r \text{holo}(r, X) \right) \\ &\quad + (-1)^k \text{conj}^{k+1} \left(\int_{b_{k+1,1}}^{b_{k+1,i}} G_{k+1}^{-1}\eta_{k+1} + r \log(r) \text{holo}(r, X) + r \text{holo}(r, X) \right). \end{aligned}$$

When $r = 0$,

$$\begin{aligned} \mathcal{F}_{3,k,i} &= (-1)^k \text{conj}^k \left(\int_{a_{k,1}}^{a_{k,i}} G_k^{-1}\eta_k \right) + (-1)^k \text{conj}^{k+1} \left(\int_{b_{k+1,1}}^{b_{k+1,i}} G_{k+1}^{-1}\eta_{k+1} \right) \\ &= (-1)^k \text{conj}^k \left(\int_{a_{k,1}}^{a_{k,i}} \frac{1}{\delta_k z} dz \right) + (-1)^k \text{conj}^{k+1} \left(\int_{b_{k+1,1}}^{b_{k+1,i}} \frac{1}{\delta_{k+1} z} dz \right) \\ &= (-1)^k \text{conj}^k \left(\delta_k^{-1} \log \left(\frac{a_{k,i}}{a_{k,1}} \right) \right) + (-1)^k \text{conj}^{k+1} \left(\delta_{k+1}^{-1} \log \left(\frac{b_{k+1,i}}{b_{k+1,1}} \right) \right). \end{aligned}$$

Thus, $\mathcal{F}_3 = 0$ and $\delta_k = 2$ for $k = 1, 2, \dots, N \Rightarrow \frac{b_{k+1,i}}{b_{k+1,1}} = \text{conj} \left(\frac{a_{k,i}}{a_{k,1}} \right)$.

7.4. Solving the equation $\mathcal{F}_4 = 0$. Using Proposition 6.3,

$$\begin{aligned} \mathcal{F}_{4,k,i} &= \frac{(-1)^k}{\sqrt{r}} \left(\overline{\int_{A_{k,i}} G^{-1}\eta - \int_{A_{k,i}} G\eta} \right) \\ &= \frac{1}{\sqrt{r}} \left[\text{conj}^{k+1} \int_{A_{k,i}} G^{(-1)^{k+1}}\eta - \text{conj}^k \int_{A_{k,i}} G^{(-1)^k}\eta \right] \\ &= \frac{1}{\sqrt{r}} \text{conj}^{k+1} \left[\sqrt{r} \left(-2\pi i \text{res}_{b_{k+1,i}} G_{k+1}\eta_{k+1} + r \text{holo}(r, X) \right) \right] \\ &\quad - \frac{1}{\sqrt{r}} \text{conj}^k \left[\sqrt{r} \left(2\pi i \text{res}_{a_{k,i}} G_k\eta_k + r \text{holo}(r, X) \right) \right] \\ &= \text{conj}^{k+1} \left[-2\pi i \text{res}_{b_{k+1,i}} G_{k+1}\eta_{k+1} + r \text{holo}(r, X) \right] \\ &\quad - \text{conj}^k \left[2\pi i \text{res}_{a_{k,i}} G_k\eta_k + r \text{holo}(r, X) \right]. \end{aligned}$$

Thus, when $r = 0$,

$$\begin{aligned} \mathcal{F}_{4,k,i} &= \text{conj}^{k+1} [-2\pi i \text{res}_{b_{k+1,i}} G_{k+1} \eta_{k+1}] - \text{conj}^k [2\pi i \text{res}_{a_{k,i}} G_k \eta_k] \\ &= 2\pi i (-1)^k \left[-\text{conj}^k (\text{res}_{a_{k,i}} G_k \eta_k) + \text{conj}^{k+1} (\text{res}_{b_{k+1,i}} G_{k+1} \eta_{k+1}) \right] \\ &= -4\pi \delta_k i (-1)^k \text{conj}^k \left(\sum_{j=1, \neq i}^{n_k} \frac{a_{k,i}}{n_k^2 (a_{k,i} - a_{k,j})} - \sum_{j=1}^{n_{k-1}} \frac{a_{k,i}}{n_k n_{k-1} (a_{k,i} - b_{k,j})} \right) \\ &\quad + 4\pi \delta_{k+1} i (-1)^k \text{conj}^{k+1} \left(-\sum_{j=1}^{n_{k+1}} \frac{b_{k+1,i}}{n_k n_{k+1} (b_{k+1,i} - a_{k+1,j})} \right. \\ &\quad \left. + \sum_{j=1, \neq i}^{n_k} \frac{b_{k+1,i}}{n_k^2 (b_{k+1,i} - b_{k+1,j})} \right) \\ &\quad + \frac{2\pi i (-1)^k}{n_k^2} (-\delta_k + \delta_{k+1}). \end{aligned}$$

We will deal with this equation further in Section 7.6 below.

7.5. Solving the Equation $\mathcal{F}_5 = 0$. Using proposition 6.4,

$$\begin{aligned} &\overline{\int_{\partial D_\epsilon(0_k)} \frac{1}{G} \eta} - \int_{\partial D_\epsilon(0_k)} G \eta \\ &= \left((-1)^k \text{conj}^{k+1} \int_{\partial D_\epsilon(0_k)} G^{(-1)^k} \eta + (-1)^{k+1} \text{conj}^k \int_{\partial D_\epsilon(0_k)} G^{(-1)^{k+1}} \eta \right) \\ &= \frac{1}{\sqrt{r}} (-1)^{k+1} \text{conj}^k \left(2\pi i \text{res}_0 \frac{1}{G_k} \eta_k + r \text{holo}(r, X) \right). \end{aligned}$$

Thus, when $r = 0$,

$$\mathcal{F}_{5,k} = 2(-1)^{k+1} \text{conj}^k (2\pi i \delta_k^{-1}) + 2\pi i = -2\pi i (2\delta_k^{-1} - 1).$$

Thus, we need $\delta_k = 2$ for $k = 1, 2, \dots, N$. This ensures that when the surfaces are scaled by $2\sqrt{r}$ the horizontal period at each end 0_k is $-2\pi i$ and at each end ∞_k is $2\pi i$. Part 7 of Proposition 8.1 confirms that the periods at the ends have the correct signs.

7.6. Uncovering the force equations and the non-horizontal period \mathcal{T}_t .

Our force equations could just be given by $\mathcal{F}_{4,k,i}$ for $k = 1, \dots, N$ and $i = 1, \dots, n_k$. However, the non-horizontal period \mathcal{T}_t whose limit is $\mathcal{T}_0 = \overline{T}$ does not have a clear relationship to the points (a, b) . Therefore, as done in [12], we will construct an isomorphism $(a, b) \mapsto (T, p, q)$.

Let $m = n_1 + \dots + n_N$. Given $p_{k,i} \in \mathbb{C}$, $k = 1, \dots, N$, $i = 1, \dots, n_k$, let $p \in \mathbb{C}^m$ be the vector whose components are $p_{k,i}$. Given $(T, p, q) \in \mathbb{C} \times \mathbb{C}^m \times \mathbb{C}^m$, define

(a, b) by

$$(3) \quad \begin{cases} a_{k,i} = (\text{conj}^k p_{k,i} q_{k,1})^{(-1)^k} \\ b_{k,i} = (\text{conj}^k p_{k-1,i} q_{k,i})^{(-1)^k} \end{cases}$$

where $p_{k+N,i} = p_{k,i} e^T$ and $q_{k+N,i} = q_{k,i}$.

Note that the way (a, b) are defined is similar to how they were defined in Proposition 7.1. We get the (a, b) in Proposition 7.1 if we let $q_{k,i} = 1$ for $k = 1, \dots, N$ and $i = 1, \dots, n_k$. Also, our (a, b) is a multiplicative version of the (a, b) in [12].

If $\delta_k = 2$ for $k = 1, \dots, N$ then

$$\begin{aligned} \mathcal{F}_{3,k,i} &= \frac{(-1)^k}{2} \text{conj}^k \left(\log \left(\frac{a_{k,i}}{a_{k,1}} \right) \right) + \frac{(-1)^k}{2} \text{conj}^{k+1} \left(\log \left(\frac{b_{k+1,i}}{b_{k+1,1}} \right) \right) \\ &= \frac{1}{2} \left(\log \left(\frac{p_{k,i}}{p_{k,1}} \right) - \log \left(\frac{p_{k,i} q_{k+1,i}}{p_{k,1} q_{k+1,1}} \right) \right) \\ &= \frac{1}{2} (\log q_{k+1,i} - \log q_{k+1,1}). \end{aligned}$$

If $\mathcal{F}_{3,k,i} = 0$ then $\log q_{k+1,i} = \log q_{k+1,1}$. Hence, $q_{k,i} = q_{k,1}$ for $k = 1, \dots, N$ and $i = 1, \dots, n_k$. Thus, let $q_k = q_{k,1}$.

We finally deal with $\mathcal{F}_{4,k,i}$. Assume $\mathcal{F}_2 = 0, \mathcal{F}_3 = 0$, and $\mathcal{F}_5 = 0$. Then,

$$\begin{aligned} \frac{\mathcal{F}_{4,k,i}}{-8\pi i} &= (-1)^k \text{conj}^k \left(\sum_{j=1, \neq i}^{n_k} \frac{a_{k,i}}{n_k^2 (a_{k,i} - a_{k,j})} - \sum_{j=1}^{n_{k-1}} \frac{a_{k,i}}{n_k n_{k-1} (a_{k,i} - b_{k,j})} \right) \\ &\quad - (-1)^k \text{conj}^{k+1} \left(- \sum_{j=1}^{n_{k+1}} \frac{b_{k+1,i}}{n_k n_{k+1} (b_{k+1,i} - a_{k+1,j})} \right. \\ &\quad \left. + \sum_{j=1, \neq i}^{n_k} \frac{b_{k+1,i}}{n_k^2 (b_{k+1,i} - b_{k+1,j})} \right) \\ &= (-1)^k \sum_{j \neq i}^{n_k} \frac{(p_{k,i} q_k)^{(-1)^k}}{n_k^2 ((p_{k,i} q_k)^{(-1)^k} - (p_{k,j} q_k)^{(-1)^k})} \\ &\quad - (-1)^k \sum_{j=1}^{n_{k-1}} \frac{(p_{k,i} q_k)^{(-1)^k}}{n_k n_{k-1} ((p_{k,i} q_k)^{(-1)^k} - (p_{k-1,j} q_k)^{(-1)^k})} \\ &\quad + (-1)^k \sum_{j=1}^{n_{k+1}} \frac{(p_{k,i} q_{k+1})^{(-1)^{k+1}}}{n_k n_{k+1} ((p_{k,i} q_{k+1})^{(-1)^{k+1}} - (p_{k+1,j} q_{k+1})^{(-1)^{k+1}})} \\ &\quad + (-1)^{k+1} \sum_{j \neq i}^{n_k} \frac{(p_{k,i} q_{k+1})^{(-1)^{k+1}}}{n_k^2 ((p_{k,i} q_{k+1})^{(-1)^{k+1}} - (p_{k,j} q_{k+1})^{(-1)^{k+1}})} \end{aligned}$$

$$\begin{aligned}
 &= \sum_{j \neq i} \frac{p_{k,i} + p_{k,j}}{n_k^2(p_{k,i} - p_{k,j})} + (-1)^k \left(\sum_{j=1}^{n_{k+1}} \frac{p_{k+1,j}^{(-1)^k}}{n_k n_{k+1} (p_{k+1,j}^{(-1)^k} - p_{k,i}^{(-1)^k})} \right. \\
 &\qquad \qquad \qquad \left. - \sum_{j=1}^{n_{k-1}} \frac{p_{k,i}^{(-1)^k}}{n_k n_{k-1} (p_{k,i}^{(-1)^k} - p_{k-1,j}^{(-1)^k})} \right) \\
 &= \sum_{j \neq i} \frac{p_{k,i} + p_{k,j}}{n_k^2(p_{k,i} - p_{k,j})} - \sum_{j=1}^{n_{k+1}} \frac{p_{k,i} + p_{k+1,j}}{2n_k n_{k+1} (p_{k,i} - p_{k+1,j})} + \frac{(-1)^k}{2n_k} \\
 &\quad - \sum_{j=1}^{n_{k-1}} \frac{p_{k,i} + p_{k-1,j}}{2n_k n_{k-1} (p_{k,i} - p_{k-1,j})} + \frac{(-1)^{k+1}}{2n_k} \\
 &= \sum_{j \neq i} \frac{p_{k,i} + p_{k,j}}{n_k^2(p_{k,i} - p_{k,j})} - \sum_{j=1}^{n_{k+1}} \frac{p_{k,i} + p_{k+1,j}}{2n_k n_{k+1} (p_{k,i} - p_{k+1,j})} \\
 &\quad - \sum_{j=1}^{n_{k-1}} \frac{p_{k,i} + p_{k-1,j}}{2n_k n_{k-1} (p_{k,i} - p_{k-1,j})}.
 \end{aligned}$$

Thus, assuming $\mathcal{F}_1 = \mathcal{F}_2 = \mathcal{F}_3 = \mathcal{F}_5 = 0$, we get $\mathcal{F}_{4,k,i} = -8\pi i F_{k,i}$. Now, if $\{p_{k,i}\}$ is a balanced configuration then define X_o as in the statement of Proposition 7.1. Because of $q_{k,i} = 1$, we get $\mathcal{F}(0, X_o) = 0$, proving the first statement of Proposition 7.1.

In order to prove the converse, assume that $\mathcal{F}(0, X) = 0$. We need to find a balanced configuration $p_{k,i}$ such that, up to some identifications, $X = X_o$ as given in Proposition 7.1. Now, $\mathcal{F}_1 = \mathcal{F}_2 = 0 \Rightarrow \alpha_{k,i} = \gamma_{k,i} = \beta_{k+1,i} = \frac{1}{n_k}$.

Choose (T, p, q) satisfying equation 3. Then $\mathcal{F}_3 = 0$ implies that $q_{k,i} = q_{k,1}$ and $\mathcal{F}_4 = 0$ implies that $p_{k,i}$ is a balanced configuration.

In order to have $X = X_o$ we need $q_{k,1} = 1$, and this requires some identifications. Note that our identifications are multiplicative versions of the corresponding identifications in Section 6.5 of [12].

Given complex numbers λ_k , let $a'_{k,i} = a_{k,i} \lambda_k$ and $b'_{k,i} = b_{k,i} \lambda_k$, and let (Σ', G', η') be the Weierstrass data corresponding to $a'_{k,i}$ and $b'_{k,i}$. Then the map $\phi : \Sigma \rightarrow \Sigma', z \in \overline{\mathbb{C}}_k \mapsto z \lambda_k$ is an isomorphism with $\phi^* G' dz = G dz$ and $\phi^* \eta' = \eta$. Thus, the Weierstrass data (Σ, G, η) and (Σ', G', η') are isomorphic and define equivalent minimal surfaces.

Hence, the following identification makes sense:

$$(a, b) \sim (a', b') \iff \forall k \exists \lambda_k \text{ such that } \forall i, a'_{k,i} = a_{k,i} \lambda_k, b'_{k,i} = b_{k,i} \lambda_k.$$

We can create similar identifications for p and q :

$$\begin{aligned}
 p' \sim p &\iff \exists \lambda \text{ such that } \forall k, i, p'_{k,i} = p_{k,i} \lambda \\
 q' \sim q &\iff \forall k \exists \lambda_k \text{ such that } \forall i, q'_{k,i} = q_{k,i} \lambda_k.
 \end{aligned}$$

As simple computations yield:

LEMMA 7.2. *The map $(T, p, q) \mapsto (a, b)$ is an isomorphism.*

Using the identifications on (a, b) , p , and q , we get that $\mathcal{F}_3 = 0 \Rightarrow q_{k,1} \sim 1$. This proves the second part of Proposition 7.1.

7.7. $D_2\mathcal{F}(0, X_0)$ is an isomorphism. The next three lemmas are from [12]. Lemmas 7.3 and 7.4 are the same as Propositions 10 and 11 in [12]. Our lemma 7.5 is partly proven in Section 6.5 of [12].

LEMMA 7.3. [12] *Let $E = \{(\alpha'_k, \beta'_k) \in \mathbb{C}^{n_k+n_{k-1}} \mid \sum \alpha'_{k,i} = \sum \beta'_{k,i} = 0\}$. The partial differential of $\mathcal{F}_{1,k}$ with respect to (α_k, β_k) is an isomorphism from E onto $\mathbb{C}^{n_k+n_{k-1}-2}$.*

Proof. See Proposition 10 in Section 6.2 of [12]. □

LEMMA 7.4. [12]

$$\sum_{k=1}^N \sum_{i=1}^{n_k} \mathcal{F}_{4,k,i}(t, X) = 0 \quad \forall(t, X).$$

Proof. See Proposition 11 in Section 6.5 of [12]. □

LEMMA 7.5. [12] *The partial differential of \mathcal{F} evaluated at $(0, X_0)$ with respect to the variables $(\alpha, \beta), \gamma, q, p, \delta$ has the form*

$$\begin{bmatrix} \mathcal{I}_1 & \cdot & 0 & 0 & 0 \\ 0 & \mathcal{I}_2 & 0 & 0 & 0 \\ \cdot & \cdot & \mathcal{I}_3 & 0 & \cdot \\ \cdot & \cdot & \cdot & \mathcal{I}_4 & \cdot \\ \cdot & \cdot & 0 & 0 & \mathcal{I}_5 \end{bmatrix}$$

with \mathcal{I}_k an invertible linear operator for $k = 1, 2, 3, 4, 5$, and so it is invertible.

Proof. The arguments explaining the first four entries of the top four rows are explained in Section 6.5 of [12]. We repeat those arguments. The key difference is that there is no fifth row or column in [12].

In the first row, \mathcal{I}_1 is invertible by Lemma 7.3. If $\alpha_k = \gamma_k$ and $\beta_k = \gamma_{k-1}$ then $\eta_k = \frac{1}{\delta_k z} G_k dz$, and so $\mathcal{F}_1 = 0$ independent of q, p , and δ . Hence, there are zeroes in the last three entries of the first row.

The second row is clear because $\mathcal{F}_{2,k,i} = \gamma_{k,i} - \gamma_{k,1}$ when $r = 0$ and is independent of α, β, q, p , and δ .

The identification on q makes \mathcal{I}_3 invertible. The zero in the third row is because \mathcal{F}_3 is independent of p .

By Lemma 7.4, we can think of \mathcal{F}_4 as a map into the subspace $\sum \mathcal{F}_{4,k,i} = 0$. Also,

$$\mathcal{I}_4 = 4\pi i(-1)^{k+1} \frac{\partial}{\partial p} F.$$

Thus, the non-degeneracy of the force equations implies that \mathcal{I}_4 is onto. The identification on p implies that \mathcal{I}_4 is invertible.

When $r = 0, \alpha_k = \gamma_k$, and $\beta_k = \gamma_{k-1}$, we get $\mathcal{F}_{5,k} = -2\pi i(2\delta_k^{-1} - 1)$. Thus, \mathcal{I}_5 is invertible. The zeroes in row five are due to the fact that \mathcal{F}_5 is independent of p and q when $r = 0, \alpha_k = \gamma_k$, and $\beta_k = \gamma_{k-1}$. □

Finally, we have shown that $D_2F(0, X_0)$ is an isomorphism, completing the proof of Proposition 7.1. There are the two free parameters $t \in \mathbb{R}$ and $T \in \mathbb{C}$. Thus, the implicit function theorems provides a three-dimensional space of solutions to the equation $\mathcal{F}(t, X) = 0$. As discussed in [3], this is the expected size of our space of minimal surfaces. Note that in [12], the surfaces are made up of domains \mathbb{C}_k . The balance configurations can be changed by complex linear transformation that do not affect the minimal surface. In our case, the domains are punctured planes \mathbb{C}_k^* , and the balance configurations can only be changed by complex multiplications. This explains the difference in the dimensions of the moduli spaces.

8. Embeddedness and Properties 2.1 and 2.2. The embeddedness proof used in [12] can be used to prove that our surfaces are embedded. The only variation is that our surfaces have pairs of ends at each level. The final detail left is showing that our surfaces satisfy Properties 2.1 and 2.2.

Let (Σ, G, η) be the Weierstrass data given by Proposition 7.1 for some small positive t . In this section, it is convenient to express ψ as

$$\psi(z) = (\text{horiz}(z), \text{height}(z)) \in \mathbb{C} \times \mathbb{R}.$$

The following proposition is essentially the same as Proposition 12 in Section 7 of [12].

PROPOSITION 8.1. *There exists a constant C , not depending on t , such that:*

(1) *For any point $z \in \tilde{\mathbb{C}}_k$ such that $\forall i, |v_{k,i}| > \epsilon, |w_{k,i}| > \epsilon$,*

$$|\text{height}(z) - \text{height}(\infty_k)| \leq C.$$

(2) *For any point $z \in \tilde{\mathbb{C}}_k$ such that $\frac{r}{\epsilon} < |v_{k,i}| < \epsilon$,*

$$|\text{height}(z) - \text{height}(\infty_k) - \frac{1}{n_k} \log |v_{k,i}(z)|| \leq C.$$

(3)

$$|\text{height}(\infty_{k+1}) - \text{height}(\infty_k) - \frac{1}{n_k} \log r| \leq C.$$

(4) Choose $P_{k,i} \in \Sigma$ such that $v_{k,i}(P_{k,i}) = \sqrt{r}$. Note that $G(P_{k,i}) = 1$. Then

$$\begin{aligned} &2\sqrt{r} (\text{horiz}(P_{k,j}) - \text{horiz}(P_{k,i})) \\ &\longrightarrow (-1)^k \text{conj}^{k+1}(a_{k,j} - a_{k,i}) = \log \overline{p_{k,j}} - \log \overline{p_{k,i}} \end{aligned}$$

and

$$\begin{aligned} &2\sqrt{r} (\text{horiz}(P_{k,j}) - \text{horiz}(P_{k-1,i})) \\ &\longrightarrow (-1)^k \text{conj}^{k+1}(a_{k,j} - b_{k,i}) = \log \overline{p_{k,j}} - \log \overline{p_{k-1,i}}. \end{aligned}$$

Thus, we can translate the surface such that $2\sqrt{r} \text{horiz}(P_{k,i}) \rightarrow \log \overline{p_{k,i}} \forall k, i$.

(5) Let $0 < \sigma < \frac{1}{2}$. The image of the domain $r^{1-\sigma} < |v_{k,i}| < r^\sigma$ converges to a catenoid with necksize $\frac{2\pi}{n_k}$, and it is contained in a vertical cylinder with radius $\frac{5r^{\sigma-1/2}}{n_k}$.

(6) The non-horizontal period of ψ is

$$\mathcal{T} = \text{Re} \int_{B_{1,1}} \phi \simeq \left(\frac{\overline{T}}{2\sqrt{r}}, \left(\sum_{k=1}^N \frac{1}{n_k} \right) \log r \right).$$

(7) For each $k = 1, \dots, N$,

$$2\sqrt{r} \text{Re}(\text{horiz}(0_k)) \longrightarrow (-1)^{k+1} \infty$$

and

$$2\sqrt{r} \text{Re}(\text{horiz}(\infty_k)) \longrightarrow (-1)^k \infty.$$

Proof. The proof of this proposition uses the same techniques used in the proof of Proposition 8 in Section 5 of [12]. □

In [12], Traizet splits \mathbb{R}^3 into the horizontal slabs

$$\text{height}(\infty_{k+1}) + \frac{\sigma}{n_{k+1}} |\log r| \leq x_3 \leq \text{height}(\infty_k) - \frac{\sigma}{n_k} |\log r|.$$

and

$$\text{height}(\infty_k) - \frac{\sigma}{n_k} |\log r| \leq x_3 \leq \text{height}(\infty_k) + \frac{\sigma}{n_k} |\log r|.$$

Traizet shows that the intersection of the first slab with $\psi(\Sigma)$ is the n_k disjoint components $C_{k,i,t}$, each one converging to a catenoid. Then, he shows that the intersection of the second slab with $\psi(\Sigma)$ is the region $E_{k,t}$, which is a graph over

the plane. The difference here is that $E_{k,t}$ is a graph over $\mathbb{C}/(2\pi i\mathbb{Z})$. Thus, our surfaces satisfy Property 2.1.

Proposition 8.1 shows that our surfaces, after scaled by $2\sqrt{r}$, satisfy Property 2.2.

DEPARTMENT OF MATHEMATICAL SCIENCES, INDIANA UNIVERSITY SOUTH BEND,
SOUTH BEND, IN 46634

E-mail: pconnor@iusb.edu

DEPARTMENT OF MATHEMATICS, INDIANA UNIVERSITY, BLOOMINGTON, IN 47405

E-mail: matweber@indiana.edu

REFERENCES

- [1] F. Baginski and V. Ramos Batista, Solving period problems for minimal surfaces with the support function, *Adv. Appl. Math. Sci.* **9** (2011), no. 1, 85–114.
- [2] C. Douglas, Doubly periodic minimal surfaces of genus 1, Ph.D. thesis, Rice University, Houston, 2008.
- [3] L. Hauswirth and M. Traizet, The space of embedded doubly-periodic minimal surfaces, *Indiana Univ. Math. J.* **51** (2002), no. 5, 1041–1079.
- [4] D. Hoffman, H. Karcher, and F. Wei, The singly periodic genus-one helicoid, *Comment. Math. Helv.* **74** (1999), no. 2, 248–279.
- [5] H. Karcher, Embedded minimal surfaces derived from Scherk’s examples, *Manuscripta Math.* **62** (1988), no. 1, 83–114.
- [6] H. Lazard-Holly and W. H. Meeks III, Classification of doubly-periodic minimal surfaces of genus zero, *Invent. Math.* **143** (2001), no. 1, 1–27.
- [7] W. H. Meeks III and H. Rosenberg, The geometry, topology, and existence of doubly periodic minimal surfaces, *C. R. Acad. Sci. Paris Sér. I Math.* **306** (1988), no. 14, 605–609.
- [8] ———, The global theory of doubly periodic minimal surfaces, *Invent. Math.* **97** (1989), no. 2, 351–379.
- [9] J. Pérez, M. M. Rodríguez, and M. Traizet, The classification of doubly periodic minimal tori with parallel ends, *J. Differential Geom.* **69** (2005), no. 3, 523–577.
- [10] W. Rossman, E. C. Thayer, and M. Wohlgemuth, Embedded, doubly periodic minimal surfaces, *Experiment. Math.* **9** (2000), no. 2, 197–219.
- [11] H. F. Scherk, Bemerkungen über die kleinste Fläche Innerhalb gegebener Grenzen, *J. Reine Angew. Math.* **13** (1835), 185–208.
- [12] M. Traizet, Adding handles to Riemann’s minimal surfaces, *J. Inst. Math. Jussieu* **1** (2002), no. 1, 145–174.
- [13] M. Weber, D. Hoffman, and M. Wolf, An embedded genus-one helicoid, *Ann. of Math. (2)* **169** (2009), no. 2, 347–448.
- [14] M. Weber and M. Wolf, Handle addition for doubly periodic scherk surfaces, *J. Reine Angew. Math.* (to appear), 2012.
- [15] F. S. Wei, Some existence and uniqueness theorems for doubly periodic minimal surfaces, *Invent. Math.* **109** (1992), no. 1, 113–136.